

EVALUATION OF THE ELECTROCHEMICAL BEHAVIOR OF PURE TITANIUM AND Ti-13Nb-13Zr ALLOY FOR USE AS BIOMATERIALS

Sérgio Luiz de Assis

IPEN/CNEN – Centro de Ciência e Tecnologia de Materiais, Caixa Postal 11049, CEP 05422-970, São Paulo, SP
slassis@ipen.br

Isolda Costa¹

IPEN/CNEN – Centro de Ciência e Tecnologia de Materiais, Caixa Postal 11049, CEP 05422-970, São Paulo, SP
icosta@ipen.br

Abstract. The electrochemical behavior of the near- β Ti-13Nb-13Zr alloy was investigated by means of potentiodynamic polarization curves and electrochemical impedance spectroscopy measurements in Hanks' solution at 37 °C. The results of the alloy were compared to those obtained for commercially pure titanium. The impedance diagrams for both, alloy and pure titanium, were interpreted using an equivalent circuit that simulates a double layer oxide composed of an inner barrier layer and an external porous layer. The inner barrier layer has been related to corrosion resistance whereas the external and porous one to osseointegration. High impedance values were obtained suggesting high corrosion resistance typical of passive materials for both tested materials in the test medium. The results also suggested the formation of a stable oxide film.

Keywords: biomaterial, Ti-13Nb-13Zr, electrochemical techniques, pure titanium.

1. Introduction

Titanium and its alloys are materials largely used for biomedical applications due to their properties of excellent biocompatibility and high corrosion resistance, comparatively to other metallic materials (Lavos-Valereto *et al.*, 2004). The high corrosion resistance of these materials is due to the formation of a protective and adherent oxide film on the metallic substrate with few nanometers thickness. This film spontaneously forms on the surface by exposure to air (Schutz and Thomaz, 1978). According to the literature (Pan *et al.*, 1996), this film has a duplex nature composed of an internal and compact barrier layer and an external porous layer. For biomedical applications a metallic material has to present high corrosion resistance since the corrosion products generated can affect the materials biocompatibility and their mechanical properties. The physiological fluids contain chlorides and therefore are corrosive to many metallic materials. The oxide film spontaneously formed on pure titanium is highly resistant to chlorides attack. However, for biomedical applications where the material is under mechanical stress, pure titanium is not convenient since it does not have high mechanical properties (Kim *et al.*, 1997). For these types of application the use of titanium alloys is indicated, once they have better mechanical properties and also present good biocompatibility and high corrosion resistance. In order to preserve biocompatibility the alloying elements used in the alloy fabrication have to be biocompatible and innocuous. One of the alloys in use for this type of application is Ti-13Nb-13Zr, which presents three of the five elements that are considered biocompatible (Ti, Nb, Zr, Ta e Pt). The chemical composition of this alloy was chosen to obtain low Young modulus, good mechanical properties and ductility (Davidson *et al.*, 1994).

In this investigation, the *in vitro* corrosion resistance of Ti-13Nb-13Zr alloy has been evaluated by electrochemical techniques in Hanks' solution. The results were compared to those of pure titanium under the same experimental conditions.

2. Experimental

The near- β Ti-13Nb-13Zr alloy and the commercially pure titanium - Ti-cp (Grade 2) were used in this investigation. The alloy titanium was laboratory prepared by Schneider (2001) by arc melting pure (99.9 %) Ti and Nb, along with Zr containing 4.5 % Hf, under argon, using a non-consumable electrode. The material was then heat-treated at 1000 °C for 1h for homogenization, water-cooled, and, subsequently, cold forged to 6.5 mm in diameter. After this latter stage, the alloy was heat-treated again. The chemical composition of the Ti alloy was determined by inductively coupled plasma atomic emission spectroscopy (ICP-AES). The composition of Ti-cp and Ti alloy used in this investigation is shown in Tab. 1.

Table 1. Chemical composition % (mass) of Ti-13Nb-13Zr alloy and pure titanium (Ti-cp)

Material	C	H	N	O	S	Hf	Fe	Nb	Zr	Ti
Ti-13Nb-13Zr	0.035	0.011	0.04	0.078	<0.001	0.055	0.085	13.18	13.49	Bal.
Titanium Grade 2	0.02	0.003	0.008	0.07	-	-	0.04	-	-	Bal.

¹ Corresponding author: IPEN/CNEN – CCTM - c.p 11049, CEP 05422-970, São Paulo, SP, icosta@ipen.br

Electrodes were prepared by epoxy cold resin mounting of both alloys, leaving areas corresponding to 0.33 cm² and 0,29 cm² for the Ti-13Nb-13Zr alloy and the pure titanium, respectively, for exposure to the electrolyte. The surfaces exposed to the electrolyte were prepared by sequential grinding with silicon carbide paper up to #2000. After polishing the surface was degreased in an ultrasonic bath for 10 minutes and then rinsed with deionized water. After surface preparation and prior to EIS tests, all the samples remained immersed for 72 h in Hanks' solution, naturally aerated at 37 °C. A three-electrode cell arrangement was used for the electrochemical measurements, with a saturated calomel reference electrode (SCE) as reference electrode and a platinum wire as the auxiliary electrode. All potentials are referred to SCE. The polarization and EIS tests were carried out in triplicate to evaluate results reproducibility. The electrolyte used to simulate the physiological medium was Hanks' solution, naturally aerated, whose composition is presented in Tab. 2. The pH of this solution is 6.8, that is, very similar to that of the physiological fluids. The temperature of test (37 °C) was controlled by a thermostatic bath, where the electrochemical cells were immersed during all test period.

Polarization was carried out using a potentiostat (EG&G PARC 273A) coupled to a computer. The investigated potential range was from -800 mV (SCE) to 3000 mV (SCE) with a scan rate of 1 mV/s. EIS tests were carried out by means of a frequency response analyser (Solartron SI-1255) coupled to a potentiostat and controlled by a software (Zplot). All EIS measurements were performed in potentiostatic mode and at the corrosion potential (E_{corr}). The amplitude of the perturbation signal was 10 mV, and the investigated frequency range varied from 10⁵ to 10⁻² Hz with an acquisition rate of 6 points per decade.

Table 2. Chemical composition of Hanks' solution

Component	Concentration (Mol/L)
NaCl	0.1369
KCl	0.0054
MgSO ₄ .7H ₂ O	0.0008
CaCl ₂ .2H ₂ O	0.0013
Na ₂ HPO ₄ .2H ₂ O	0.0003
KH ₂ PO ₄	0.0004
C ₆ H ₁₂ O ₆ .H ₂ O	0.0050
Red phenol 1%	0.0071
pH	6.8

3. Results

The potentiodynamic polarization curves for Ti-13Nb-13Zr and commercially pure titanium (Ti-cp) after 72 h of immersion in Hanks' solution naturally aerated and at 37 °C are shown in Fig. 1. The corrosion potential (E_{corr}) estimated from the polarization curves were -380 mV (SCE) and -360 mV (SCE), for Ti-13Nb-13Zr and Ti-cp, respectively.

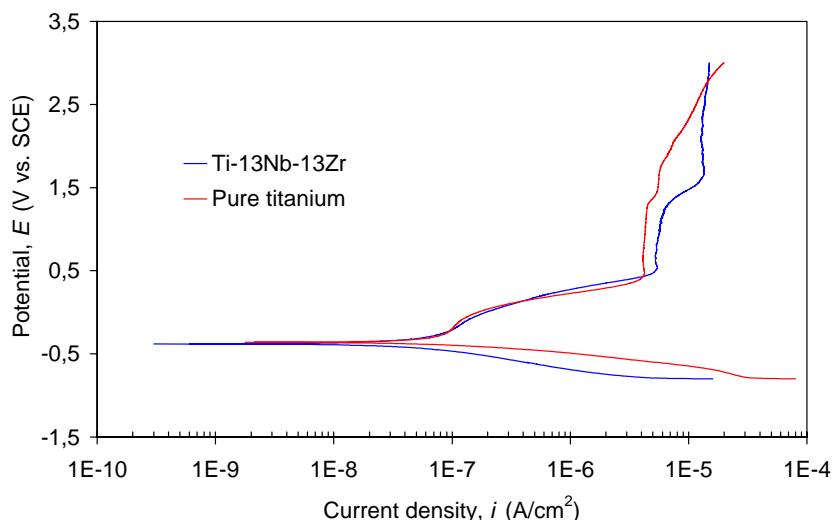


Figure 1. Potentiodynamic polarization curves for Ti-13Nb-13Zr and Ti-cp after 72 h of immersion in Hanks' solution naturally aerated solution at 37 °C. Scanning rate: 1mV/s.

The anodic current density continuously increases with potential for low overpotentials, i.e., close to the corrosion potential (E_{corr}), up to potentials of approximately 500 mV (SCE) for Ti-cp and 550 mV (SCE) for Ti-13Nb-13Zr. At these last potentials, the potential does not show any significant change with the potential up to 1300 mV (SCE), indicating a passive potential range, but from 1300 mV (SCE) it increases again with the potential. This increase in potential was faster for the Ti-13Nb-13Zr alloy comparatively to Ti-cp. The mean corrosion current densities (i_{corr}) and corrosion potential (E_{corr}) obtained from the polarization curves are shown in Tab. 3 for both studied materials. The i_{corr} values were estimated by extrapolating the cathodic curve to the corrosion potential. The very low values obtained are typical of passive materials.

Table 3. Mean values of corrosion potential (E_{corr}) and corrosion current density (i_{corr}) for Ti-13Nb-13Zr alloy and Ti-cp after 72 h of immersion in naturally aerated Hanks' solution at 37 °C. The values inside parenthesis indicated the standard deviation of the data. The number of data used to estimate standard deviation was 3 (N=3).

Ti-13Nb-13Zr		Ti-cp	
E_{corr} mV(SCE)	i_{corr} nA/cm ²	E_{corr} mV(SCE)	i_{corr} nA/cm ²
-411.2	29.4	-343.9	27.1
(45.7)	(17.7)	(15.9)	(7.9)

Figure 2 shows the Bode diagrams (Z modulus and phase angle) for Ti-13Nb-13Zr and Ti-cp at E_{corr} , for 72 h of immersion in Hanks' solution. The results show phase angles close to -90 ° from medium to low frequencies indicating a highly capacitive response, typical of passive metals. An equivalent electric circuit was proposed in the literature (Pan *et al.*, 1996) to fit the results of titanium alloys in simulated physiological fluids and this is shown in Fig. 3. The experimental results of this study and of the fitting to the proposed equivalent circuit are shown in Figs. 4 and 5. According to the proposed model, the oxide film on titanium and its alloys has a duplex nature composed of an inner and continuous barrier layer and an external porous layer. In the EIS diagrams, the results at high frequencies are related to the porous layer, whereas the barrier layer response is related to the data obtained from medium to low frequencies (Assis *et al.*, 2005) In the proposed model of Fig. 3, R_b and CPE_b represent the resistance and capacitance of the barrier layer, and R_p and CPE_p , the resistance and capacitance of the porous layer, respectively. R_s is the ohmic resistance, mainly due to the electrolyte.

The constant phase element (CPE) of the proposed equivalent circuit represents the deviation from an ideal capacitor. The impedance of the CPE is given by $Z_{CPE} = [C(j\omega)^n]^{-1}$, where $-1 \leq n \leq 1$. The n value is related to a non-uniform current distribution due to surface irregularities, such as rugosity and defects. As the n value approaches 1 the behavior approximates that of an ideal capacitor.

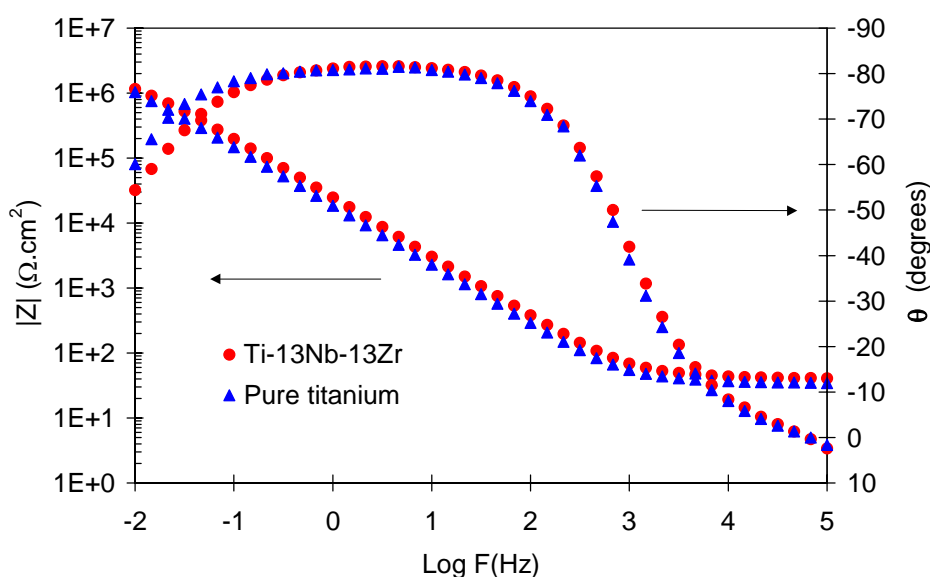


Figure 2. Bode spectra for Ti-13Nb-13Zr and Ti-cp after 72 h in naturally aerated Hanks' solution at 37 °C. Data obtained at the E_{corr} .

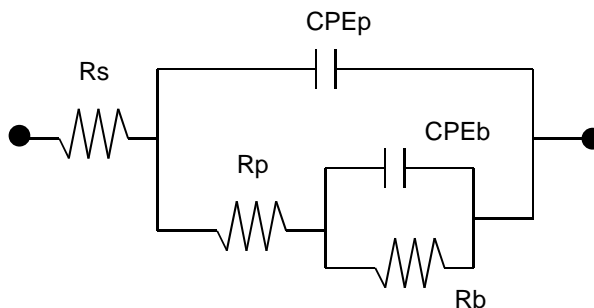


Figure 3. Equivalent electric circuit proposed to fitting the experimental results obtained for Ti-13Nb-13Zr and Ti-cp after 72 h in naturally aerated Hanks' solution at 37 °C.

Table 5 shows the resistance and capacitance values for the porous and barrier layers, estimated from fitting the experimental results to the equivalent circuit shown in Fig. 3.

Table 5. Resistance and capacitance values for the porous and barrier layer, obtained from fitting of experimental results to the equivalent circuit shown in Fig. 3. The chi-squared values are represented by χ^2 .

Material	Rs	CPEp	Rp	CPEb	Rb	χ^2
	($\Omega \cdot \text{cm}^2$)	($\mu\text{F}/\text{cm}^2$)	($\Omega \cdot \text{cm}^2$)	($\mu\text{F}/\text{cm}^2$)	($\text{M}\Omega \cdot \text{cm}^2$)	
Ti-cp	35	9.4	111	0.9	2.8	4.3E-4
Ti-13Nb-13Zr	41	7.1	115	0.7	2.3	9.8E-4

The very low values of χ^2 (order of 10^{-4}), indicate a good quality of the fitting to the equivalent circuit proposed and this is supported by the results presented in Fig. 4 and 5.

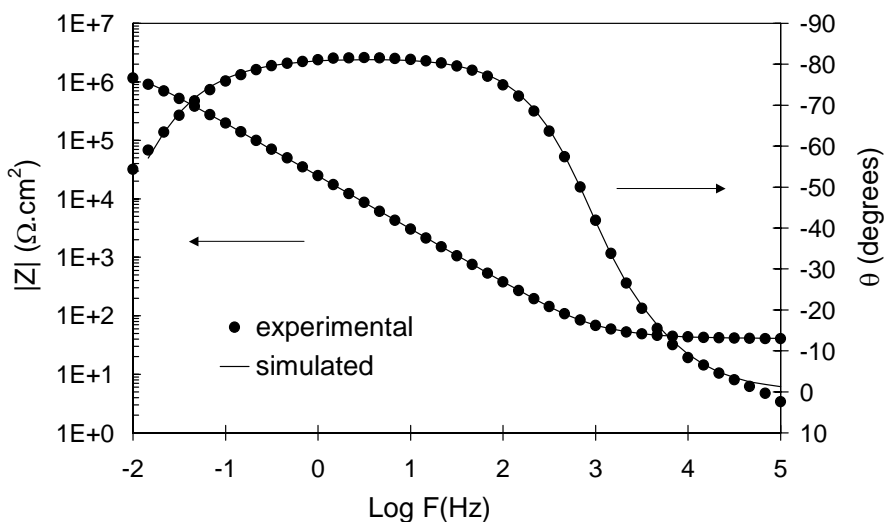


Figure 4. Bode diagrams of experimental and simulated data from fitting to proposed equivalent circuit for Ti-13Nb-13Zr alloy after 72 h of immersion in naturally aerated Hanks' solution at 37 °C.

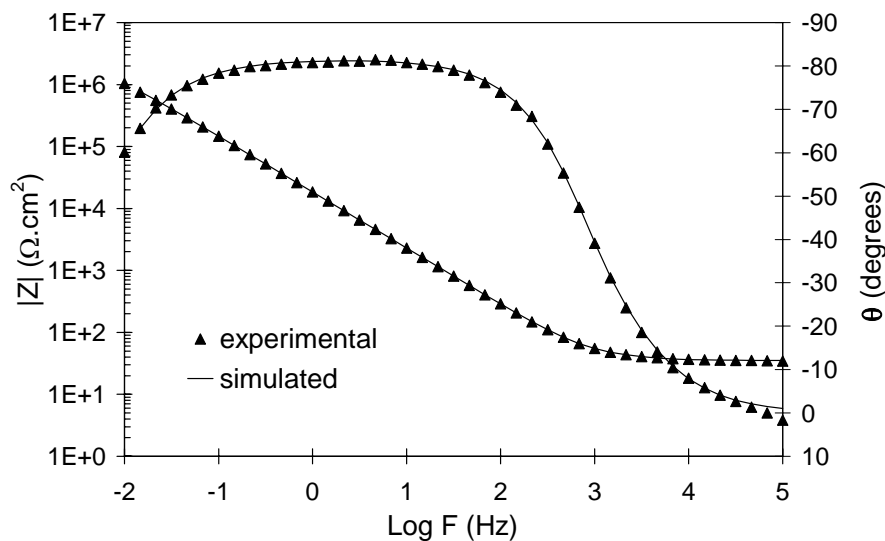


Figure 5. Bode diagrams of experimental and simulated data from fitting to proposed equivalent circuit for Ti-cp after 72 h of immersion in naturally aerated Hanks' solution at 37 °C.

4. Discussion

The polarization curves obtained show a behavior typical of transition from the immunity to the passive region. The increase in current density with the potential from the corrosion potential (E_{corr}) until potentials around 500 mV (SCE), is likely due to the insufficient increase in oxide thickness with potential to compensate the increase in potential. This current increase could also be caused by the oxidation of TiO and Ti₂O₃ to TiO₂ (Yu and Scully, 1997). Subsequently, the oxide thickening apparently compensates the increase in potential and there is a potential range where the current does not change with potential. The current increases again at potentials around 1300 mV (SCE) and this could be related to the formation of titanium compounds with components from Hanks' solution (Lavos-Valereto *et al.*, 2002). The Pourbaix diagram (potential vs. pH) for Ti-H₂O (Pourbaix, 1974) shows that in nearly neutral solutions, the following species, in this order, Ti, TiO, Ti₂O₃ and TiO₂, become stable with the increase in potential. This observation supports the hypothesis of a transition from the immunity to the passive region.

The EIS results showed largely capacitive results and high impedance values in the medium to low frequency region (order of 10⁶ Ω.cm²), indicating a high corrosion resistance of the tested materials. The Bode diagrams (phase angle and Z modulus), show two distinct regions: (a) a high frequency region (1-100 kHz), where the Z modulus is stable and close to 0°, indicating a resistive behavior due to the ohmic resistance, mainly due to the solution, R_s , between the reference and the tested material, and (b) from medium to low frequencies, phase angles close to -90°, i.e., highly capacitive, that decreases at lower frequencies. The high capacitive results are typical of passive and protective oxide films (González *et al.*, 1999). The impedance results for Ti-cp and Ti-13Nb-13Zr after 72 h immersion in naturally aerated Hanks' solution 37 °C were analysed using the equivalent circuit of Fig. 3 and the Z_{view} software. The results obtained for the various components of the proposed model are shown in Tab. 4. It can be seen that the barrier layer resistance (R_b) is considerably higher (factor of 10⁴) than the porous one, (R_p). This result suggests that the corrosion protection is provided mainly by the barrier type layer, whereas the porous one has no significant effect on the corrosion resistance of the tested material. According to the literature (Lavos-Valereto *et al.*, 2004 and Pan *et al.*, 1998) the porous layer is mainly associated to osseointegration, helping it by allowing the incorporation of components from the physiological medium into the pores of this layer. The incorporation of species such as calcium and phosphate from the physiological medium leads to the formation of hydroxyapatite, with composition similar to that of the bone.

5. Conclusion

The high resistance values associated to the barrier layer comparatively to that of the porous one, indicate that the corrosion resistance of Ti-cp and Ti-13Nb-13Zr alloy is mainly due to the thin and compact inner layer formed directly on these materials. The polarization curves indicated a passive behavior for both Ti-cp and Ti-13Nb-13Zr alloy in naturally aerated Hanks' solution at 37 °C showing very low current densities (order of nA/cm²) at the corrosion potential and a very high resistance to the breakdown of the passive film.

6. Acknowledgements

The authors are grateful to S.G. Schneider for providing the Ti-13Nb-13Zr alloy used in this investigation.

7. References

- Assis, S.L., Rogero, S.O., Antunes, R.A., Padilha, A.F. and Costa, I., 2005, "A Comparative Study of the In Vitro Corrosion Behavior and Cytotoxicity of a Superferritic Stainless Steel, a Ti-13Nb-13Zr Alloy, and an Austenitic Stainless Steel in Hanks' Solution", *Journal Biomedical Materials Research*, 73B, pp.109-116.
- Davidson, J.A., Mishra, A.K., Kovacs, P. and Poggie, R.A., 1994, "New Surface-Hardened Low-Modulus Corrosion Resistant Ti-13Nb-13Zr Alloys for Total Hip Arthroplasty", *Bio-medical Materials and Engineering*, 4, pp.231-243.
- González, J.E.G., and Mirza-Rosca, J.C., 1999, "Study of the Corrosion Behavior of Titanium and Some of its Alloys for Biomedical and Dental Implant Applications", *Journal of Electrochemical Chemistry*, 471, pp.109-115.
- Kim, T.I., Han, J.H., Lee, I.S., Lee, K.H., Shin, M.C. and Choi, B.B., 1997, "New Titanium Alloys for Biomaterials: A study of Mechanical and Corrosion Properties and Cytotoxicity", *Bio-Medical Materials and Engineering*, 7, pp. 253-263.
- Lavos-Valereto, I.C., Costa, I. and Wolyneec, S., 2002, "The Electrochemical Behavior of the Ti-6Al-7Nb Alloy with and without Plasma-Sprayed Hydroxyapatite Coating in Hanks' Solution", *Journal Biomedical Materials Research*, 63, pp. 664-670.
- Lavos-Valereto, I.C., Wolyneec, S., Ramires, I., Guastaldi, A.C. and Costa, I., 2004, "Electrochemical Impedance Spectroscopy Characterization of Passive Film Formed on Implant Ti-6Al-7Nb Alloy in Hanks' Solution", *Journal of Materials Science in Medicine*, 15, pp. 55-59.
- Pan, J., Liao, H., Leygraf, C., Thierry, D. and Li, J., 1998, "Variation of Oxide Films on Titanium Induced by Osteoblast-Like Cell Culture and the Influence of an H₂O₂ Pretreatment", *Journal Biomedical Material Research*, 40, pp.244-256.
- Pan, J., Thierry, D. and Leygraf, C., 1996, "Electrochemical Impedance Spectroscopy Study of the Passive Oxide Film on Titanium for Implant Application", *Electrochimica Acta*, 42, 7/8, pp. 1143-1153.
- Pourbaix, M., 1974, "Atlas of Electrochemical Equilibria in Aqueous Solutions, National Association of Corrosion Engineers, pp. 217-222.
- Schneider S.G., 2001, "Obtenção e Caracterização da liga Ti-13Nb-13Zr para aplicação como Biomaterial", Tese (Doutorado), Instituto de Pesquisas Energéticas e Nucleares, São Paulo, Brasil.
- Schutz, R.W. and Thomas D.E., 1978, "Corrosion of Titanium and Titanium Alloys", *Metals Handbook*, 9th Metals Park, Ohio, ASM international, 13, pp. 669-706.
- Yu, S.Y. and Scully, J.R., 1997, "Corrosion and passivity of Ti-13%Nb-13%Zr in Comparison to Other Biomedical Implant Alloys", *Corrosion*, 53, 12, pp. 965-976.

8. Responsibility notice

The authors are the only responsible for the printed material included in this paper.